Hindawi
Advances in Polymer Technology
Volume 2023, Article ID 8835940, 18 pages
https://doi.org/10.1155/2023/8835940

*Review Article*

# A Review on Hydrogen Generation by Photo-, Electro-, and Photoelectro-Catalysts Based on Chitosan, Chitin, Cellulose, and Carbon Materials Obtained from These Biopolymers

**Sajjad Keshipour, Mina Hadidi, and Ozra Gholipour**

*Department of Nanotechnology, Faculty of Chemistry, Urmia University, Urmia, Iran*

Correspondence should be addressed to Sajjad Keshipour; s.keshipour@urmia.ac.ir

Received 31 March 2023; Revised 30 May 2023; Accepted 6 July 2023; Published 25 July 2023

Academic Editor: Jun Ling



Biopolymer-based catalysts like chitosan, chitin, and cellulose offer sustainability and high efficiency both as the catalyst or catalyst support in a broad range of applications, especially in hydrogen evolution reactions. This review focused on hydrogen evolution catalysts of chitosan, chitin, cellulose, and carbon materials obtained from these biopolymers to highlight the opportunities of these sustainable catalysts in this field. All the reports in this area could be classified as one of the photocatalysts, electrocatalysts, and photoelectrocatalysts, and their mechanisms were clarified in the beginning. Then, the results of catalysts obtained from each of these biopolymers were discussed separately to reveal the roles of the biopolymers. It was concluded that all of the biopolymers enjoy some common benefits like hydrogen bonding, chelating with transition metals, easy chemical modification, high performance, and potential to be used as the precursors of carbon or porous materials. Among them, chitosan showed outstanding merit due to the better performance in metal grafting, amendment, and ability of hydrogen bonding. Moreover, it provides highly active nitrogen-doped carbon as the support of transition metals in the hydrogen generation, enhancing the reaction rate by retarding the charges recombination.

## 1. Introduction

While currently utilizing fossil fuels in most industries is inevitable, environmental issues created by these combustions force companies to develop new systems operating with green fuels like hydrogen [1, 2]. This gas is a promising fuel considering its high potential energy and relatively safe combustion product [3, 4]. A substantial number of publications on hydrogen generation procedures demonstrate that an efficient protocol has not been stabilized yet [5, 6]. In this regard, a wide variety of starting materials were used for the hydrogen production, such as water, formic acid, hydrazine, and boranes, especially by heterogeneous catalysts [7]. Since the reusability of the catalyst is considered a notable characteristic of the hydrogen production reaction, heterogeneous catalysts gained significant attention to promote the reaction [8]. Sustainability is of importance for the heterogeneous catalysts, leading to the employment of natural-based supports, such as cellulose (Cel), chitin, and chitosan (CS), in the chemical transformations [9, 10].

Recent century has witnessed superior growing up in the uses of sustainable polymers, in which biopolymers are the center of concentrations due to the abundancy, availability, inexpensive nature, easy modification, and nontoxicity [11]. Cel is a well-known biopolymer on account of broad applications such as production in paper, veterinary nutrients, cosmetics, wears, and drugs [12–14]. CS and chitin are the other utilitarian biopolymers, especially in biomedical such as wound healing, drug delivery, and vaccine delivery [15]. All of the mentioned biopolymers demonstrated attractive behavior to be used as heterogeneous supports of various catalysts. Easy modification of these polymers has been led to numerous reports about modification of them by transition metals. Cel, chitin, and CS could adsorb metal cations efficiently because of many heteroatoms on their structure; in particular, CS and chitin with nitrogen atoms quickly complex with metals like Pd, Pt, Co, and Au. The obtained

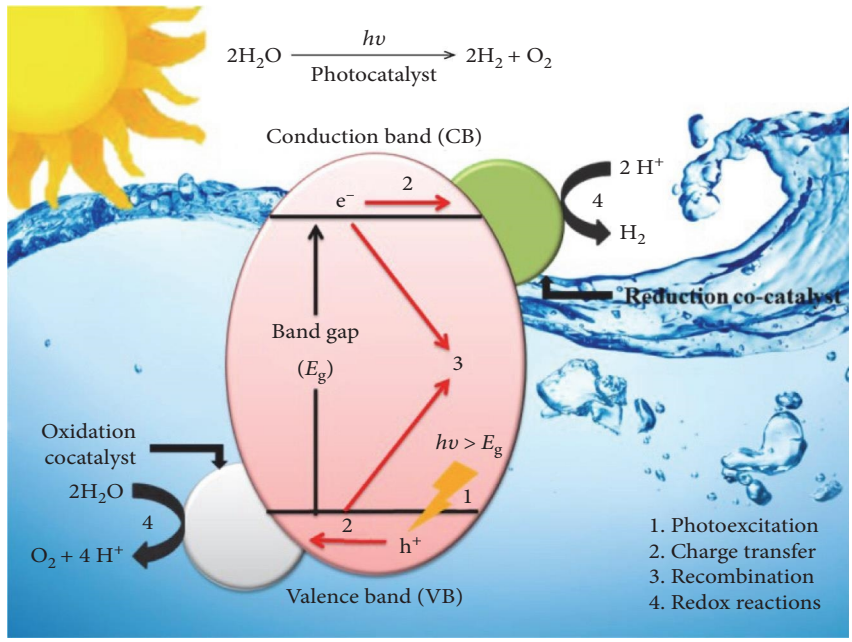


Figure 1: Mechanism of the photocatalytic water splitting.

composites could provide catalytical clean hydrogen production [16]. Herein, we pointed out all the catalysts synthesized from CS, chitin, and Cel in the hydrogen production reactions. This survey is of significant importance because it provides a comprehensive review research on hydrogen production by catalysts obtained from chitin, Cel, and CS, highlighting their strengths and weaknesses. To provide a better insight, four main subjects were followed in the separate sections, including hydrogen generation, CS, chitin, and Cel. After elucidation of the hydrogen production by various pathways, the capabilities of materials constructed by these biopolymers were highlighted in hydrogen evolution. In each section, all the reports in the area were discussed with a leading focus on the feature of the biopolymer affording the high activity. This paper can provide a valuable overview on the advantages and disadvantages of different approaches and guide to the developing more efficient and sustainable hydrogen production methods.

## 2. Hydrogen Production

Hydrogen is a clean and renewable energy carrier that has the potential to play a significant role in the transition to a low-carbon economy. There are various methods for the hydrogen production, such as steam reforming, gasification, and electrolysis. However, some of these methods use natural pollutant sources, such as natural gas or coal, as feedstock, resulting in carbon emissions and other environmental impacts. These methods are classified as blue and gray, which are considered unsustainable approaches for hydrogen production [17–19]. On the other hand, there is a green method for the hydrogen evolution, which is based on photocatalytic [20, 21], electrocatalytic [22, 23], and photoelectrocatalytic techniques [24, 25]. These methods use renewable energy sources, such as solar energy or wind power, in a sustainable and ecofriendly way to split water. As a result, these nonfossil fuel-based methods are considered the best approaches for the hydrogen production [26].

Photocatalytic reactions enjoy a free source of energy without employing high-cost instrumentation, which leads to the significant extension in various applications. Therefore, this is not surprising that hydrogen generation was also benefits from the photocatalytic systems to afford a worthy energy source in a green manner. The mechanism of photocatalytic hydrogen production involves photo absorption, producing electron–hole, and reduction of $H^+$ to $H_2$. The photocatalyst absorbs light energy, in the form of ultraviolet, visible light, or infrared, which excites electrons from the valence band to the conduction band to generate electron–hole pairs. The injected electrons are in charge of hydrogen evolution from protons by a catalyst. The role of semiconductors to accelerate this phenomenon is vital, leading to a wide study on the development of efficient nanocomposites as the semiconductors. Moreover, the semiconductor could prevent a quenching process by the retarding charges recombination (Figure 1) [27–30].

Electrocatalytic water splitting is a process that uses an electrocatalyst to facilitate the separation of water into hydrogen and oxygen gases. The electrocatalytic water splitting initiated with the formation of charges on the electrode surface. Water is electrolyzed in an electrochemical cell, which consists of an anode and a cathode separated by an electrolyte. A voltage is applied across the electrodes, which causes water to split into hydrogen at the cathode and oxygen at the anode. The electrode reactions involved are as follows:

$$\text{Cathode}: 2H^+ + 2e^- \longrightarrow H2, \tag{1}$$

$$\text{Anode}: 2H_2O \longrightarrow O_2 + 4H^+ + 4e^-. \tag{2}$$

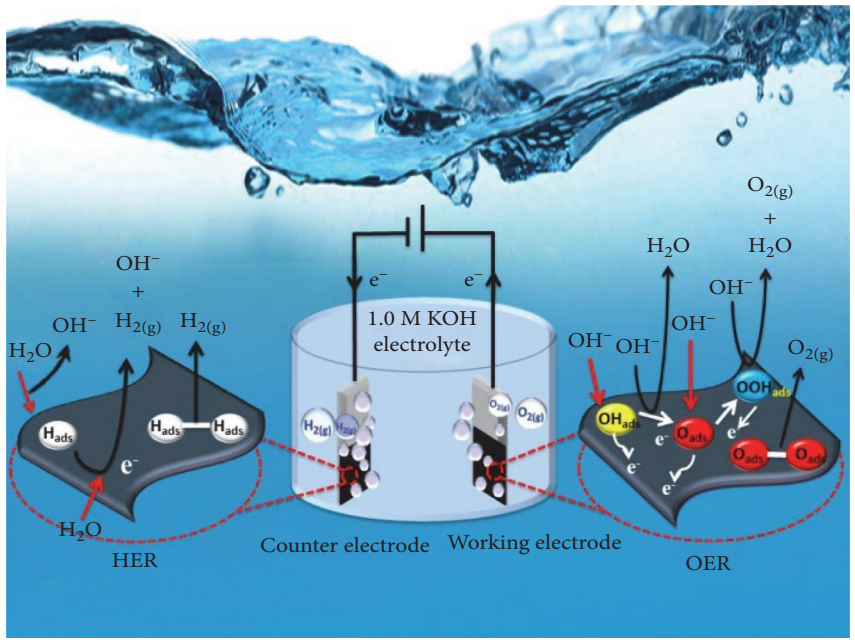


Figure 2: Mechanism of the electrochemical water splitting.

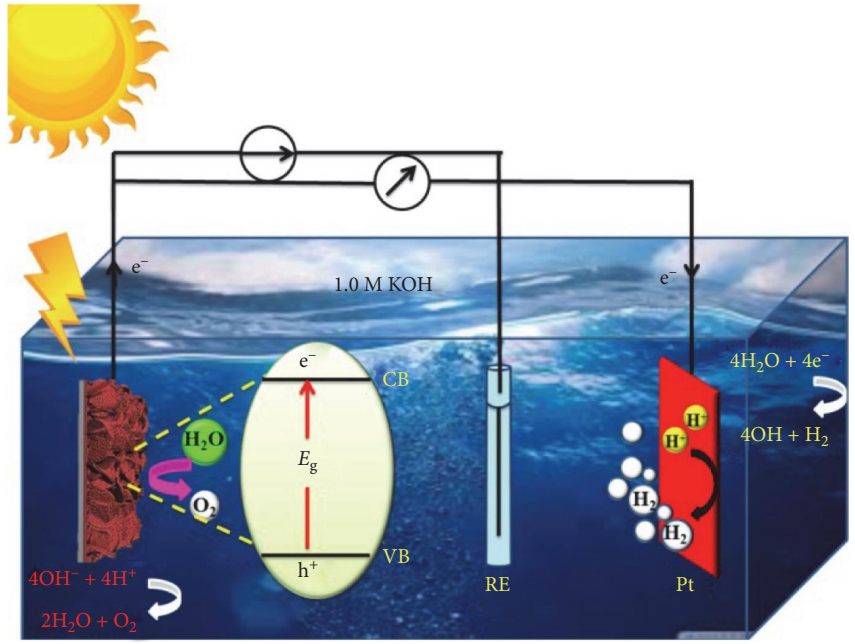


Figure 3: Mechanism of the photoelectrochemical water splitting.

An electrocatalyst is used to facilitate the electrode reactions and improve the efficiency of the process. The electrocatalyst minimizes the activation energy and subsequently increases the rate of the overall reaction (Figure 2) [31–34].

Photoelectrocatalytic water splitting is a process that combines photocatalysis and electrocatalysis to split water into hydrogen and oxygen gases driven by solar energy on the surface of active electrodes. A photocatalyst, typically a semiconductor material such as titanium dioxide ($TiO_2$) or a metal oxide, absorbs photons from sunlight and makes electron–hole pairs in the material. The excited electrons move to the conduction band, while the holes formed in the valence band. The electrons and holes are separated and migrate to the surface of the photocatalyst. The cathode and/or anode are typically coated with an electrocatalyst to improve the electrode reactions and improve the efficiency of the process. At the cathode, the excited electrons reduce water molecules to $H_2$ and hydroxyl, and on the other side, the holes oxidize water molecules to form $O_2$ and protons (Figure 3).

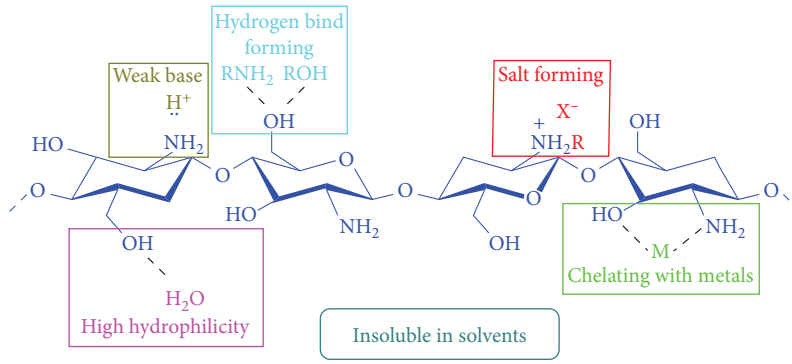


Figure 4: CS structure and some of its features.

Table 1: Most important factors and reports of CS on the hydrogen generation reactions.

| Entry | Effect | Catalyst | Hydrogen production rate | Tafel slope ($mV\ dec^{-1}$) | Current density ($mA\ cm^{-2}$) |
|---|---|---|---|---|---|
| 1 | As a weak base | CS hydrogel/pencil graphite [45] | 2,050 ($ml\ g^{-1}\ min^{-1}$) | – | – |
| 2 | | Poly(vinyl) alcohol/CS [46] | 1,277 ($ml\ H_2\ L_{cat}^{-1}\ day^{-1}$) | – | – |
| 3 | Chelating CS with metals | CS-supported Pd NPs [16] | 24.76 ($mol\ H_2\ (molPd)^{-1}\ min^{-1}$) | – | – |
| 4 | | CS-Co complex [47] | 30,258 ($\mu\ mol\ g^{-1}\ hr^{-1}$) | – | – |
| 5 | | Cu-Co/CH [48] | 1,370 ($ml\ g^{-1}\ min^{-1}$) | – | – |
| 6 | Retardant of charge recombination in semiconductors and photocorrosion inhibitor | Cu@CS–LN [49] | $2.5 \times 105$ ($\mu mol\ gCu^{-1}\ hr^{-1}$) | – | – |
| 7 | | Pt-CS-$TiO_2$ [50] | 93.46 ($\mu mol\ hr^{-1}$) | – | – |
| 8 | Easy chemical modification | Pd (0)/GO-ILCS-$Fe_3O_4$ [51] | 30.2 ($mol\ H_2\ (mol_{Pd}\ min^{-1}$) | – | – |
| 9 | | rGO/carboxymethyl CS [52] | 480 ($min^{-1}$) | – | – |
| 10 | Hydrogen bonding | Polypyrrole-CS/Au NPs [53] | – | −152 | 6.12 |
| 11 | | PPy/$Bi_2MoO_6$/CS [54] | – | 19.16 | – |
| 12 | | Polyaniline-CS/Pt [55] | – | 121 | 10.76 |
| 13 | | $g$-$C_3N_4$/CS/Au [56] | – | 13 | 6.01 |
| 14 | | $g$-$C_3N_4$/BN@CS [57] | – | 150 | – |
| 15 | As the precursor of carbon material in hydrogen evolution | $Mo_2C$ QD/NGCL [58] | – | 98.1 | 10 |
| 16 | | ZnO@AC NPs [59] | 1,257.69 ($ml\ g^{-1}\ min^{-1}$) | – | – |
| 17 | | CoO-CdS [60] | 10.60 ($mmol\ g_{cat}^{-1}\ hr^{-1}$) | – | – |
| 18 | As a template for the synthesis of catalysts | $Co_3O_4$ macrocubes with CS template [61] | 1,497.55 ($ml\ g_{cat}^{-1}\ min^{-1}$) | – | – |

Overall, photoelectrocatalytic water splitting combines the advantages of photocatalysis and electrocatalysis to generate hydrogen and oxygen gases using solar energy [35–39].

## 3. CS

CS, a linear polysaccharide constructed from randomly distributed $\beta$-linked d-glucosamine and $N$-acetyl-d-glucosamine, has gained attention in the energy conversion, such as fuel cells, due to some characteristic properties (Figure 4) [40, 41]. This biopolymer application domain is rapidly increasing in the energy field like hydrogen generation due to the characteristic properties like insolubility in most of the solvents, weak base behavior, hydrophobicity, hydrogen bonding, complexation with metals, and organic salts formation [42–44].

Table 1 summarized significant features of CS which affected its performance in the hydrogen generation reaction, and the results in this area were listed. In continue, we studied the impacts of each of these factors in detail.

Most of the reports on using CS-based catalysts are around its modified form with the transition metals. However, the metal-free CS was used for the hydrogen generation at a mercury and amalgam electrode. This reaction indicated a significant dependence on the buffer concentration and pH with the high performances in concentrated solutions at low pHs [62]. While the mechanism of the hydrogen evolution did not investigate in this work, we believe that the protonation of amine

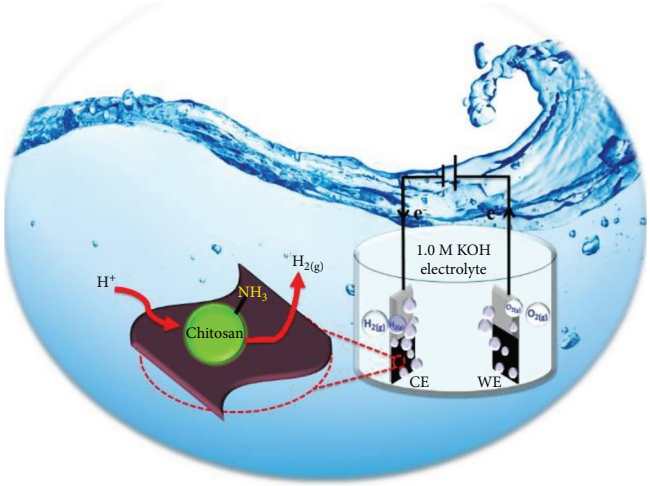


Scheme 1: Effect of amine and amide groups of support in proton evolution reaction.

groups of CS as a weak base in acidic media is a prelude for the evolution of protons to $H_2$. Therefore, CS directly impressed the transformation reaction of $H^+$ to $H_2$, in which $H^+$ is prepared to the evolution after binding with amines of the biopolymer. Although the assessment about consuming nonbonding electrons of CS's amine in the transformation of proton to $H_2$ is not established, but the impact of the base behavior of CS was approved when the hydrogen evolution reaction did not proceed by a chitin oligomer (containing *N*-acetylated glucosamines). It is worthy to note that in the chitin structure, nitrogen atoms are arranged in the amide moiety with no basic behavior to bind with protons (Scheme 1).

The CS hydrogel entrapped pencil graphite composite (CH/PG) was also employed in the hydrogen generation *via* an electrochemical pathway with the rate of 2,050 ml $g^{-1}$ $min^{-1}$. This catalyst can be simply prepared and also recycled by taking hydrogel from the reaction mixture [42]. In another work, a two-chamber microbial electrolysis cell, separated by a poly (vinyl) alcohol/CS membrane, was utilized for the production of hydrogen with a rate in the range of 1,277 ± 46 ml $H_2$ $L_{cat}^{-1}$ $day^{-1}$. The catalytic activity of composite was found close to Nafion in the hydrogen generation reaction. The efficiency of the prepared composite was also investigated as a membrane that demonstrated the highest acetate removal of 7% [45].

Amine groups have the potential to be anchored to unoccupied orbitals of transition metals *via* nonbonding electrons. This stabilizing interaction has been widely employed to the deposition of transition metals on various natural and synthetic polymers. Abundance amine groups on the CS backbone makes the biopolymer a susceptible support of transition metals to afford catalysts for diverse transformations like hydrogen evolution. Remarkable numbers of amine functionality on CS inhibited aggregation of metal nanoparticles (NPs), providing desirable conditions for the uniform fine-size formation of transition metals on the polymer [15]. For instance, fine particles of Pd with the particle size 4–8 nm were deposited on CS to obtain CS-supported Pd NPs as a catalyst for the decomposition of $NH_3BH_3$ through a

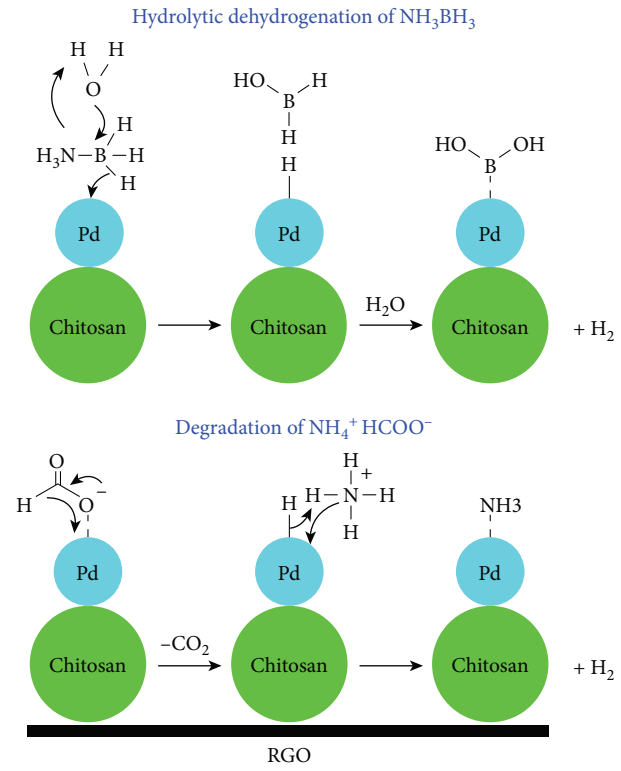


Scheme 2: Mechanisms of hydrogen generations from Pd-catalyzed hydrolysis of $NH_3BH_3$ and degradation of $NH_4^+HCOO^-$.

hydrolytic dehydrogenation (Scheme 2). As a result, the catalytic reaction in 0.81 and 0.45 of $NH_3BH_3$ provided $E_a$ of 36.25 kJ $mol^{-1}$ with a maximum turnover frequency (TOF) of 24.76 mol $H_2$ $mol_{Pd}^{-1}$ $min^{-1}$ at 303 K [46]. After that, researchers have managed to obtain a high dispersion value of uniformly sized Pd NPs on CS-graphene oxide (GO) beads by adsorption of $Pd(NH_3)_4^{2+}$ followed by a reduction stage utilizing $NaBH_4$ in order to the synthesize Pd/CS-GO catalyst for the hydrogen production from ammonium formate degradation (Scheme 2). Among their findings were reported to be no $CO/CH_4$ formed during the process.

Another noteworthy outcome was the fact that Pd average size reached over 3 nm after three cycles due to the leaching and caused deactivation of the catalyst [63]. In continue, a one-pot strategy was employed to fabricate the CS-Co complex as a catalyst for the hydrogen generation in a photoelectrochemical pathway. The amount of hydrogen production was determined up to 30,258 $\mu$mol $g^{-1}$ $hr^{-1}$ under the best conditions [47]. The nanocomposite of CS and Co NPs was electrochemically coated on a bare 316 l stainless steel alloy to afford a catalytic system for hydrogen generation from calcium hydrogen phosphate solution. The acquired results have confirmed the efficiency of the nanocomposite in the electrochemical corrosion resistance of the walls as well as promoting the hydrogen production rate [64]. This is a clear document to highlight the promising ability of CS in the supporting of transition metals since remarkable stability is needed for the corrosion inhibition by a composite. As mentioned, this gift resulted in the amine functionalities' strong

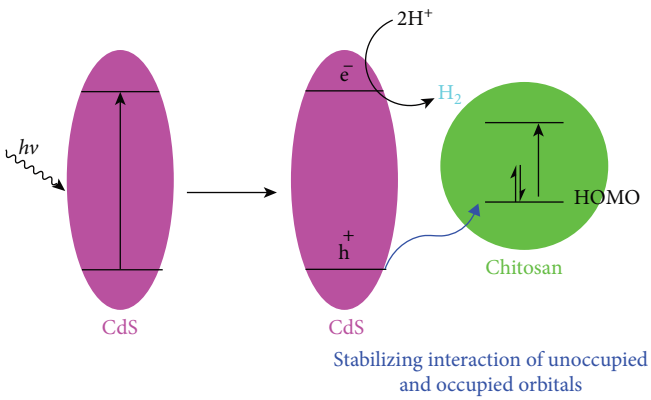


FIGURE 5: Stabilization of holes generated in CdS by HOMO electrons of CS.

interactions with metals. A growth in yields was observed for the bimetallic systems supported on CS. Bimetallic NPs entrapped CS hydrogel container (Cu–Ag/CH, Cu–Co/CH, Cu–Ni/CH) was prepared and used for the $H_2$ generation. The results showed that Cu–Co/CH was more efficient in hydrogen production with the rate of 1,370 ml $g^{-1}$ $min^{-1}$ of $H_2$, while Cu–Ni/CH is efficient in the removal of toxic contaminants. The major advantage of this catalyst is its superior activity and cost-effective nature. It should be highlighted that the selection of metals is vital in the yield [48].

Semiconductors are powerful tools for the progress of photocatalytic reactions, in which they trap the photon energy and generate excited electrons and holes to accelerate the redox reactions. The most important issue about the semiconductors is the fast recombination of electron–hole pairs before use in the reaction. This concern could be suppressed by the addition of various retardants like graphene compounds. CS–CdS xerogel composite was prepared to look for a catalytic system to hydrogen evolution suppressing the previous issues, including rapid recombination of electrons–holes produced from photo-irradiation. It was demonstrated that migration of holes from the semiconductor to the highest occupied molecular orbital (HOMO) of CS, created by the nonbonding electrons of hydroxyl and amine groups, led to a remarkable retarding in the charges quenching (Figure 5). Furthermore, photo corrosion is a common issue for the CdS semiconductor, which is resulted from the accumulation of electrons–holes or species created from electrons–holes on the semiconductor. The presence of CS spatially inhibited from the charges contact achieved by the amines and hydroxyl groups. This benefit led to the stability of the photocatalytic reaction for 55 hr [65].

Lignin was also employed to bind with CS for the synthesis of a framework for the metal NPs by the formation of core–shell material. Solubility of the biopolymers in acidic media, and precipitation of them by changing pH allows to trapping hosts in their network. CS–lignin (C–LN) carbon framework bio-composite-encapsulated Cu catalyst (Cu@CS–LN) was employed in methanol reforming. The Cu@CS–LN produced $2.5 \times 10^5$ $\mu$mol $H_2$ $g_{Cu}{}^{-1}$ $hr^{-1}$, which is two times higher than Cu@CS [49]. A similar observation

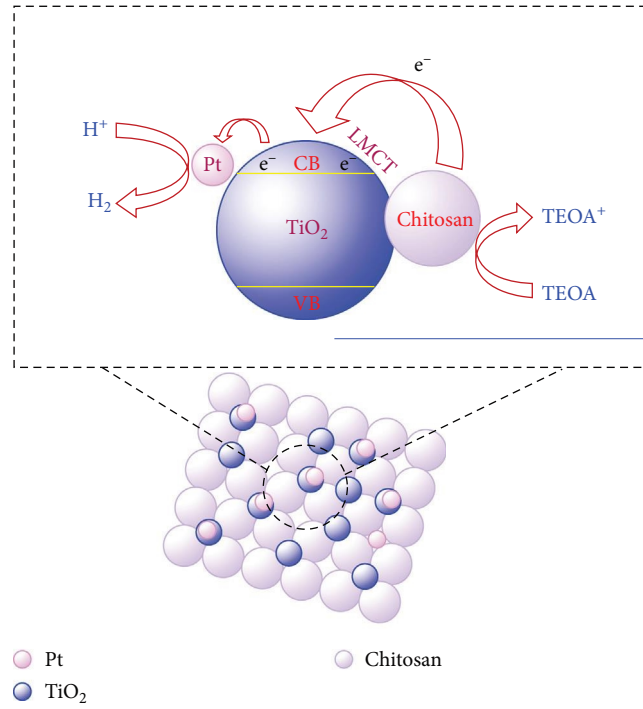


SCHEME 3: Schematic illustration of photocatalytic hydrogen production over Pt-CS-$TiO_2$ catalyst.

was also reported for the composite of Pt-CS-$TiO_2$ photocatalyst, in which the CS as a ligand injected electrons to $TiO_2$, retarding electron–hole recombination. The photocatalyst can produce $H_2$ with a high rate of 280.4 $\mu$mol in 3 hr, because of charge transfer complex between CS and $TiO_2$ (Scheme 3) [50].

Amine species have been known for their superior nucleophilic properties, leading to the innumerable substitution reactions by the nucleophilic substitutions. Possessing amines, CS hosts new functionalities by nucleophilic substitutions [66]. In this type of reaction, a leaving group on the electrophilic compound is replaced by a CS's amine. Modification of CS with ionic liquid 3 afforded ionic liquid grafted CS (ILCS) by an $S_N2$ reaction (Scheme 4). This reaction was proceeded by the attack of highly nucleophilic amine to the carbon-containing Br and a C–N bond formation simultaneously leaving the Br. The reaction of ILCS with GO gave a composite which under deposition of Pd NPs gave an organometallic catalyst. Obtained results suggested the high catalytic activity, and excellent reusability in the hydrolytic decomposition of $NH_3BH_3$ towards hydrogen generation. TOF was determined to be as high as 25.6 mol $H_2$ $mol_{Pd}{}^{-1}$ $min^{-1}$. Notably, the $E_a$ of the reaction over the resultant catalyst was negligible (38 kJ $mol^{-1}$) compared to most of the Pd-based catalysts, offering easy progressing the reaction [51]. In continue, ILCS, GO, ferrous chloride, and ferric chloride were used as precursors to produce magnetic composites to investigate their hydrogen evolution as catalysts. In this study, authors benefited from a one-pot synthesis method combined with coprecipitation and then, utilized GO-ILCS-$Fe_3O_4$ composite as the support of Pd NPs. Although their findings exhibited no enhancement in the

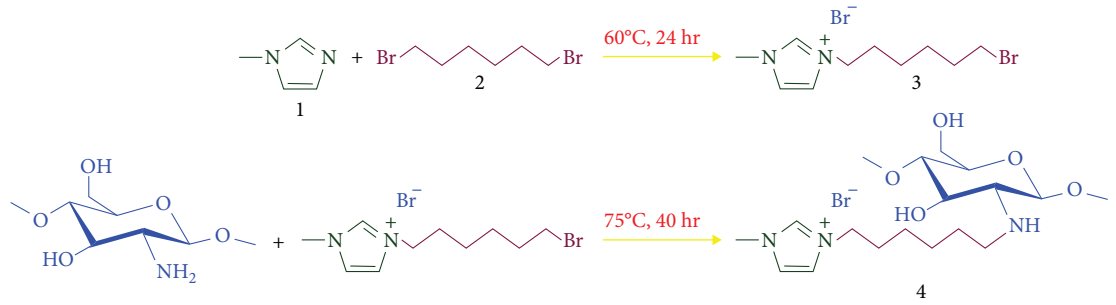


Scheme 4: Preparation of ILCS.

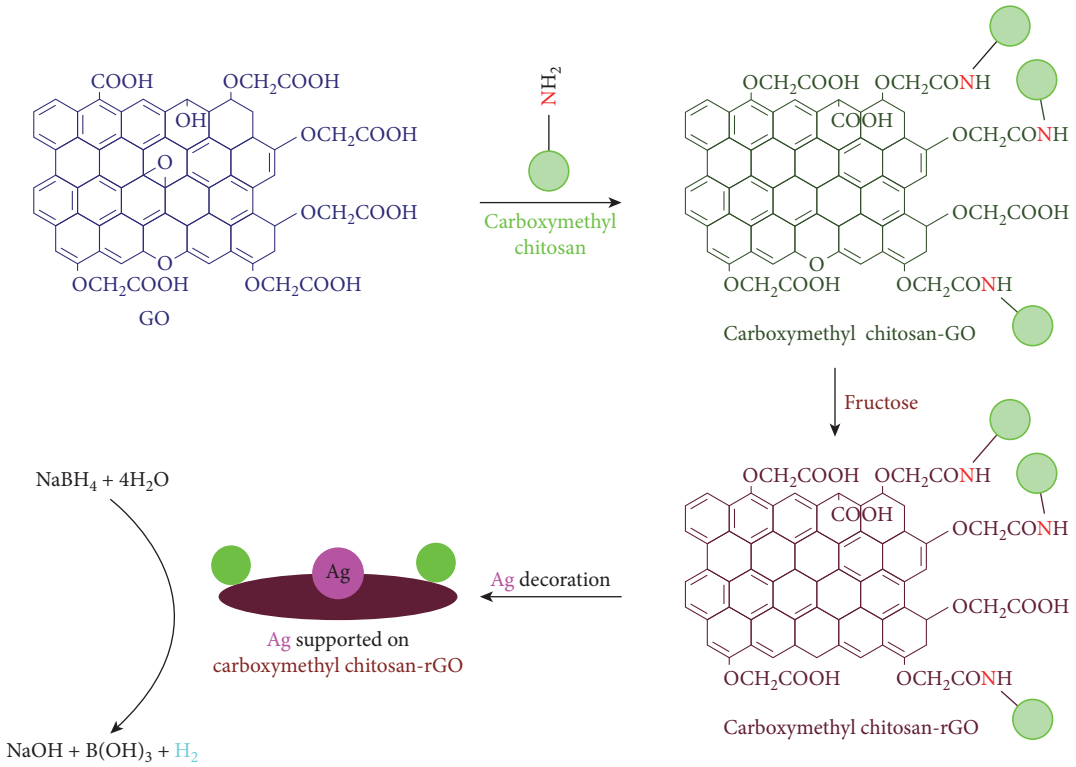


Scheme 5: Preparation of electrode of rGO/carboxymethyl CS.

hydrogen generation from $NH_3BH_3$ (TOF up to 25.2 mol $H_2$ $mol_{Pd}^{-1}min^{-1}$) compared to the previous report, a significant positive in the easy magnetically separation and reusability of Pd/GO-ILCS-$Fe_3O_4$ was achieved [51]. The amidation reaction could provide strong binds between the CS and the catalyst. The reaction of tetracarboxylic acid functionalized Co(II)-phthalocyanine with chitosan by amidation reaction in the presence of carboxylic acid activators led to the formation of a photocatalyst with a bandgap of 1.71 eV and TOF of 510 $hr^{-1}$ for water splitting [41].

In recent years, reduced GO (rGO) promoted a significant number of catalytic reactions, in particular, in the field of energy conversion due to notable characteristics such as biocompatibility, easy production, high surface area, easy modifications, insolubility, easy cycling, and so on [67]. Quadrado and Fajardo [52] used a combination of rGO and carboxymethyl CS for supporting Ag NPs to prepare a new catalyst for hydrogen generation through a straightforward borohydride decomposition reaction (Scheme 5). Synthesis of rGO/carboxymethyl CS was carried out by the amidation reaction between N–H of carboxymethyl CS and carboxylic acid of GO and then, reduction of GO to rGO by fructose (Scheme 2). This catalyst was demonstrated remarkable catalytic activity in hydrogen production (maximum rate of $180 \times 102$ ml $min^{-1}$ $g^{-1}$), achieving TOF value of 480 $min^{-1}$. This composite indicated a superior activity in both aqueous and nonaqueous systems and recyclability for several times without any significant decrease in the yields [52].

CS has outstanding hydrophilicity owning hydroxyl and amine groups by the ability of hydrogen bonding with water. Hydrogen bonding potential of CS was considered as a propitious capacity to perch other compounds on the polymer. Polypyrrole is an example of compound by abundant N–H bonds susceptible for the hydrogen bonding, which was loaded on the

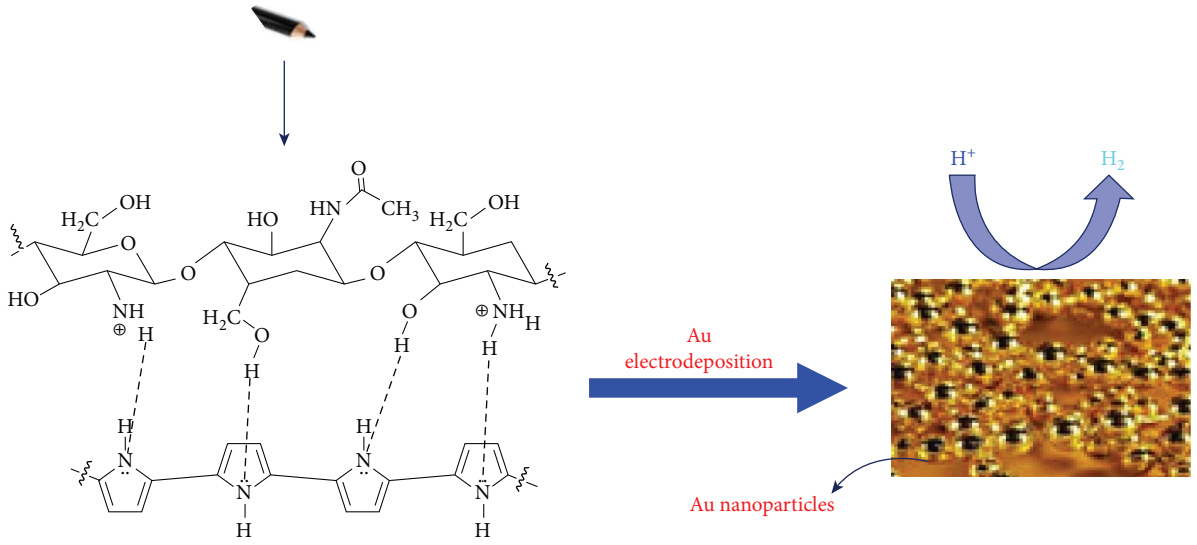


Scheme 6: Preparation of electrode of polypyrrole-CS/Au NPs.

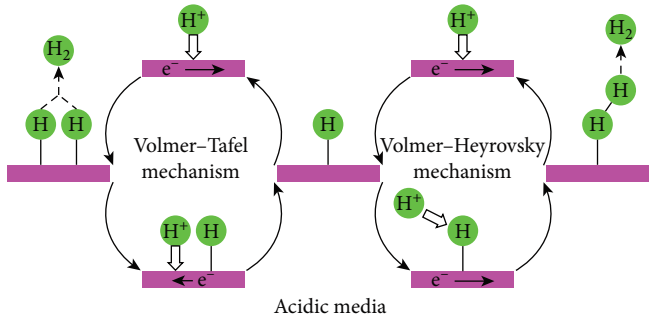


Scheme 7: Volmer–Tafel and Volmer–Heyrovsky mechanisms for the hydrogen evolution in acidic media.

CS *via* this interaction. A graphite electrode was prepared by polypyrrole-CS/Au NPs to furnish an electrocatalyst for the hydrogen production from a water-splitting reaction. For obtaining the catalyst, the electrode was modified potentiometrically with polypyrrole in the presence of CS and subsequent deposition of Au NPs (Scheme 6). Polypyrrole has a notable conductivity with the wide applications for improving the composites conductivities stocked on the electrodes. Hydrogen bonding efficiently connected the synthetic polymer to CS, leading to a stable catalyst on the electrode. Moreover, the strategy offered a pathway to suppress the costs *via* using minimum amounts of Au. Electrochemical data indicated that the thickness of the loaded catalyst impressed the electron transfer rate, which finally affected the current densities [53].

In a similar study, an aluminum electrode containing Au deposited on polypyrrole-CS was obtained *via* coelectrodecoration of polypyrrole and CS on the electrode and then Au loading by cyclic voltammetry. CS also provided the possibility of the polymer interconnection and high dispersion of Au NPs on the composite. High dispersion of Au was found as a remarkable point to increase the desired reaction in a high cathodic current density and reduce the Tafel slope to $-152\ \text{mV dec}^{-1}$ and current density of $6.12\ \text{mA cm}^{-2}$. This finding demonstrated that Volmer–Heyrovsky mechanism is in charge of the transformation, in which the Volmer reaction controls the rate (Scheme 7). Furthermore, the stability of the catalyst was confirmed as it was reusable over 8 hr [68]. $Bi_2MoO_6$ as an inexpensive precursor instead of Au in the composite with polypyrrole/CS accommodated electrochemical hydrogen production with the low Tafel slope of $19.16\ \text{mV dec}^{-1}$. This success in the yield was also attributed to the high surface area, in which the exfoliated morphology enhanced the surface area [54].

Polyaniline has the potential of polypyrrole in the hydrogen bonding with CS, in which strong interactions are created between them, and also the conductivity of the CS is improved in the presence of this conductive polymer. An electrocatalyst was constructed from the loading of Pt NPs on a pencil graphite electrode containing a composite of polyaniline-CS. This electrocatalyst performance was found to be more promising in the field of hydrogen generation at low pHs with the Tafel slope of $121\ \text{mV dec}^{-1}$ and current density of $10.76\ \text{mA cm}^{-2}$. The mechanism of the reaction was studied by an electrochemical method, indicating the Volmer–Heyrovsky route. The present composite can be an intangible proof for the hydrogen evolution regarding that the kinetics of the reaction was desired when the conductivity was enhanced by polyaniline [55].

Nasri et al. [56] prepared an efficient nanocatalyst from graphitic carbon nitride (g-$C_3N_4$), CS, and Au NPs through a

convenient, green, and cost-effective method. In this reaction, pyrolysis of urea and laser ablation of Au solution afforded g-$C_3N_4$ and Au NPs, respectively, which their mixing with CS gave g-$C_3N_4$/CS/Au. Hydrogen bonding between nitrogen atoms of g-$C_3N_4$ and N–H of CS was in charge of connecting two organic materials. Synthesized catalyst after electrochemically coating on a stainless-steel mesh was employed in the hydrogen generation reaction with the Tafel slope of 13 mV $dec^{-1}$ and current density of 6.01 mA $cm^{-2}$. Cyclic voltammetry demonstrated the high activity of the nanocomposite in the degradation reaction [56]. Hydrogen evolution reaction was carried out with the graphitic carbon nitride (g-$C_3N_4$) integrated with boron nitride (BN) and CS (g-$C_3N_4$/BN@CS nanocomposite). The as-synthesized material shows superior stability for 20 hr and HER performance with an overpotential of ~520 mV and a Tafel slope of 150 mV $dec^{-1}$ [57].

CS is considered the promising starting material of the N-doped carbon compounds, having the benefits of easy transformation, inexpensive nature, abundancy, and sustainability. This reaction was employed to synthesis of N-doped graphite as a support of $Mo_2C$ quantum dots. Decoration of nanometer scales of quantum dots of $Mo_2C$ on the sheets of N-doped graphite through solid-phase reaction gave an active composite for hydrogen generation with the Tafel slope of 98.1 mV $dec^{-1}$, current density of 10 mA $cm^{-2}$, and overpotential of ~136 mV. This reaction was impressed by the synergistic effects of catalyst ingredients in the water-splitting. The presence of nitrogen with a long-pair electron created an interaction with an unoccupied level of $H^*$, leading to the efficient decomposition of water (Scheme 1). Furthermore, N as the heteroatom increased available electrons on Mo and Cel atoms, in which these electrons conducted on the water-splitting reaction [58]. Activated carbon obtained from CS-supported zinc oxide NPs (ZnO@AC NPs) was used for hydrogen evolution with a yield of 1,257.69 ml $min^{-1}$ $g^{-1}$. Hydrogen production reusability tests revealed 85% catalytic activity for the recycled ZnO@AC NPs and high stability and selectivity [59].

CS-derived carbon-supported CoO-CdS photocatalyst was reported to produce 10.60 mmol $g_{cat}{}^{-1}$ $hr^{-1}$ of $H_2$, which is 7.21 times higher than that of pure CdS, with high stability and quantum efficiency. The photocatalysts showed remarkable performance by retarding the charge recombination and migration photogenerated carries. This is ascribed to the formation of z-scheme heterojunction between carbon-supported CoO nanorods and CdS [60].

Porous macro-cubes structures of $Co_3O_4$ catalysts were constructed from the blending CS, urea, and cobalt(II) under hydrothermal conditions. The next step was involved with the calcination of extracted solids at different temperatures for 4 hr. This research was conducted to obtain a new heterogeneous catalytic system of $Co_3O_4$, in which CS provided the template for the creation of a porous structure of the catalyst, and urea was the support. Considerable high hydrogen evolution was provided by the catalyst with a rate of up to 1,497.55 ml $H_2$ $min^{-1}$ $g_{cat}{}^{-1}$. The ratio of the ingredients used in the catalyst synthesis was impressed the size and thickness of macrocubes, and their performance [61]. A high catalytic activity of $Co_3O_4$ resulted in a high surface area of the catalyst caused by the utilization of CS template.

## 4. Chitin

Chitin is an abundant biopolymer in the nature, which is composed of *N*-acetylglucosamine. This biopolymer is employed for the large-scale production of CS through a deacetylation reaction. Therefore, chitin offers most of the features of CS, such as biocompatibility, complexation with metals, insolubility in solvents, hydrophobicity, weak base activity, and formation of organic salts [69]. However, acetylated amines in the chitin backbone substantially reduce the biopolymer intense for the modifications by nucleophilic reactions, leading to the more attention to CS than chitin, especially in the hydrogen generation reactions. Our literature study revealed that chitin-based catalysts have not been well studied for the hydrogen evolution, and reports on this area are rare. Table 2 summarizes significant features of chitin that impressed its activity in the hydrogen generation reaction, and the reported works in these areas were shown. In continue, we studied the impacts each of these factors in detail.

Anchoring with metals enterprise is conceivable for the chitin on account of the plenty of amide functionalities. Amides demonstrated superior activity to complex with the transition metals as the bidental ligands (O=C–N). By dispersing chitin in a Ru(III) solution and subsequent reduction of the cation, the nanocomposite of chitin/Ru NPs was obtained to be employed in the hydrogen generation reactions. This catalyst demonstrated superior activity in the hydrogen production from hydrolysis of $NaBH_4$ with the rate of up to 55.29 l $g_{Ru}{}^{-1}$ $min^{-1}$ at 30°C with the $E_a$ of 39.16 kJ $mol^{-1}$. Surprisingly, Ru supported on chitin remained stable for 20 cycles with a negligible decrease in the yield, indicating the notable capability of chitin amides in the anchoring of metal NPs [70].

Although chitin-supported catalysts for hydrogen evolution are not well established, the use of this inexpensive biopolymer deserved the synthesis of carbon material for supporting metal catalysts in the energy conversion. In a report, chitin was used as a precursor of N-doped carbon nanofibers, in which the adsorbing Pt on chitin, freeze–drying the prepared composite, and its final pyrolysis led to the formation of a high surface area composite of carbon-Pt. This composite revealed a significant activity towards hydrogen evolution with an overpotential of 34 mV and a Tafel slope of 39 mV $dec^{-1}$, values worthy than commercial Pt/C (36 and 35 mV $dec^{-1}$) [71]. Pyrolysis of chitin in the presence of cobalt salt created a porous structure containing Co, N, and S when the product of high-temperature thermal treatment finally was sulfurized. This catalyst promoted oxygen reduction, oxygen evolution, and hydrogen generation reactions successively (Scheme 8). Researchers synthesized active species of Co catalyst due to the defects made in the catalyst structure by the etching step. Furthermore, S and N-doped in the crystalline network create multiple active sites. For the hydrogen

Table 2: Most important factors and reports of chitin on the hydrogen generation reactions.

| Entry | Chitin role | Catalyst | Hydrogen production rate | Tafel slope (mV $dec^{-1}$) | Overpotential (mV) |
|---|---|---|---|---|---|
| 1 | As a ligand | Chitin/Ru NPs [70] | 55.29 ($l\,min^{-1}$ $g_{Ru}{}^{-1}$) | – | |
| 2 | As the precursor of porous supports | Carbon-Pt [71] | – | 39 | |
| 3 | | Co/CoO [72] | 12.63 ($mmol\,g^{-1}\,hr^{-1}$) | – | |
| 4 | | Ru@NC [73] | – | – | 39 |
| 5 | | N-doped carbon nanofibers [71] | – | 39 | 34 |
| 6 | | Porous structure containing Co, N, and S [72] | – | – | 264 |

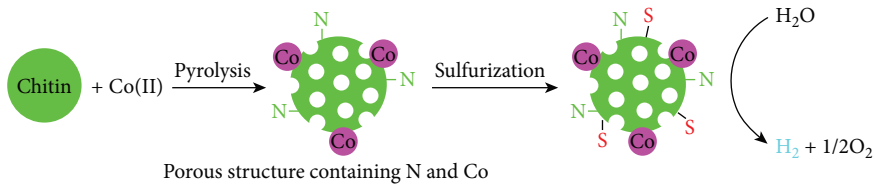


Scheme 8: Synthesis of porous structure containing Co, N, and S from chitin for water-splitting.

evolution reaction, a current density of 10 mA $cm^{-2}$ with an overpotential of 264 mV was obtained [72]. A sustainable and cost-effective catalyst of chitin-derived carbon and Co/CoO hybrid was synthesized *via* precarbonization of chitin and cobalt nitrate under nitrogen and subsequent calcination. This simple pathway afforded an invaluable catalyst for the hydrogen evolution of triethanolamine (TEOA) solution in the presence of Eosin Y as a photosensitizer with the rate of 12.63 mmol $g^{-1}$ $hr^{-1}$. It was demonstrated that Co/CoO retards the recombination of electron–hole pairs generated by photo-irradiation, leading to the efficiently enhances in the reaction rate. On the other hand, nitrogen atoms improved the reaction rate due to the hydrophilicity [72].

In another work, Ru NPs anchored on chitin-derived porous nitrogen-doped carbon (Ru@NC) are produced and used for HER. Ru@NC shows HER overpotential of 39 mV at 10 mA $cm^{-2}$, with high stability in alkaline solution. The well HER performance of Ru@ NC is due to small particle size, changing electronic structure of Ru by N doping, and a strong metal–support interaction [73].

## 5. Cellulose

The most accessible biopolymer in the nature, Cel, is a polysaccharide constructed from a linear chain of several hundred $\beta$-linked d-glucose units [74]. A bunch of structural forms have been reported for the polymer, such as microcrystalline C, Cel nanofibril, hairy Cel nanocrystalloids, spherical NPs of Cel, and aerogel Cel obtained from acid hydrolysis [75], mechanical processing [76], thermal treatment [77], enzymatic hydrolysis [78], and freeze–drying of Cel [79], respectively. Each of these states offers different applications since they have unique features. These materials attracted the attention of researchers in the energy field for the catalytic purposes. Table 3 indicates an important characteristic of cellulose affecting its activity in the hydrogen evolution, and the reported works in this subject were highlighted. In continue, we investigated the effect each of these factors in detail.

Spherical NPs of Cel with the size of 210 nm were synthesized in a new pathway *via* heating microcrystalline Cel or sawdust under a pressure of 600 psi. The BET analysis revealed a surprising aspect ratio for the formed Cel NPs as 1,500 $m^2\,g^{-1}$. The yield of NPs formation indicated time-dependent with the better results in a long time. This synthesized nanomaterial was utilized in the electrochemical generation of hydrogen, and it was found that the pretreatment method did play a remarkable role in the activation of NPs for proceeding with electrochemical hydrogen evolution [93]. A porous lamellar membrane was made using bismuth oxychloride (BiOCl) nanosheets and CS nanofibers (CSFs) via self-assembly. Interestingly, the as-prepared BiOCl/CSFs afforded a hydrogen production rate of 12.49 $\mu mol\,g^{-1}\,hr^{-1}$. The hybridization of CSFs with 2D lamellar membranes helps nanochannel size, water transport, and mechanical strength (Scheme 9) [80].

Nano-fibrillated Cel (NFC) has been known as a high surface area nanomaterial, enjoying biocompatibility and abundancy [94]. The capability of NFCs was examined as a carrier of $TiO_2$ NPs as semiconductors for the photocatalytic water-splitting, in which it was recognized that the NFC-$TiO_2$ composite has a superior activity in hydrogen production up to 265 $\mu mol\,g^{-1}\,min^{-1}$, exceeding two to five times over the pristine $TiO_2$ [81]. A literature survey on the C-$TiO_2$ composites revealed a significant finding about their interaction, in which the Cel surface could be covered by $TiO_2$ molecules by a long-range electrostatic interaction and hydrogen binding (Figure 6) [95]. Recently, Cel nanocrystals were modified with $TiO_2$ *via* a one-pot strategy to reach a chiral nematic photoactive structure. Self-assembly of the

Table 3: Most important factors, and reports of cellulose on the hydrogen generation reactions.

| Entry | The desired effect | Catalyst | Hydrogen production rate ($\mu$mol g$^{-1}$ hr$^{-1}$) | Tafel slope (mV dec$^{-1}$) | Overpotential (mV) |
|---|---|---|---|---|---|
| 1 | High surface area | BiOCl/CSFs [80] | 12.49 | – | |
| 2 | Electrostatic and hydrogen bonding | NFC–TNPs [81] | 265 | – | |
| 3 | | CNC/$TiO_2$ [82] | 287.2 | – | |
| 4 | | NFC@$Fe_3O_4$@TNP [83] | 436 | – | |
| 5 | | Pt@HN-BC [84] | – | −35 | |
| 6 | Support of transition metal-based compounds | Cel hydrogel-Ni [85] | 489.2 | – | |
| 7 | | Ni-P/BC [86] | – | 141 | 161 |
| 8 | | Cu@CC | $3.35 \times 10^6$ | – | |
| 9 | | CdS/10%BC-$Mo_2S$ [87] | 20,020 | – | 154 |
| 10 | Cellulose/Cel as a precursor of catalysts for hydrogen generation | CoO@N/S-CNF [88] | – | 32 | −55 |
| 11 | | N, S-doped carbon nanofibers coated with N, P-doped carbon NPs [89] | – | 99 | |
| 12 | | CNFs/$CoSe_2$ [90] | – | 54 | 119 |
| 13 | | Berry-shaped-CdS/$Mo_2S$ [91] | 63,590 | – | |
| 14 | | C-doped graphitic carbon nitride [92] | 1,024 | – | |

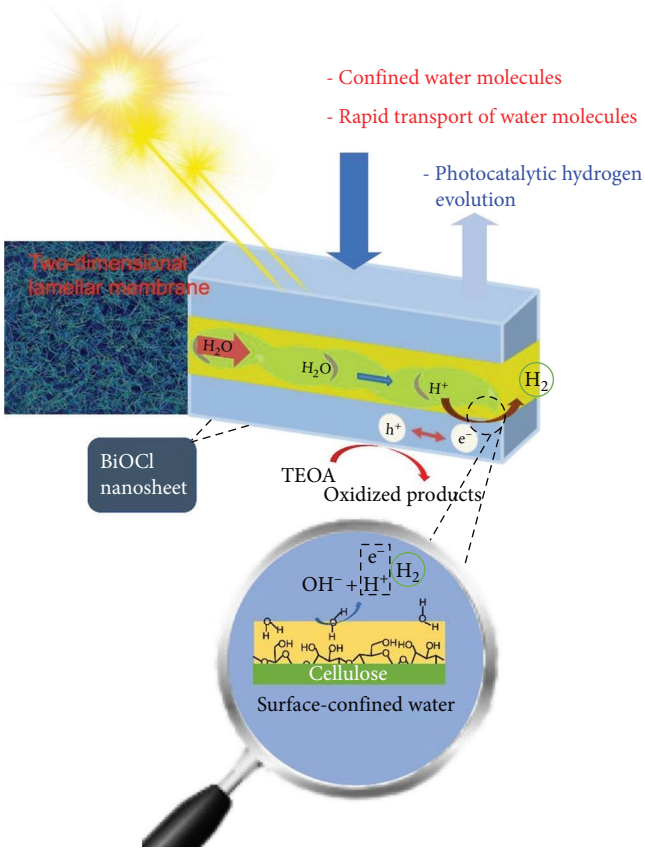


Scheme 9: Photocatalytic hydrogen evolution mechanism of BiOCl/CSFs.

nanofibers provided a chiral nematic structure with the evaporation of the solvent, which formed a xerogel template for $TiO_2$ NPs. Moreover, a lamellar form of $TiO_2$ was generated with calcination of the obtained xerogel structure, which promoted

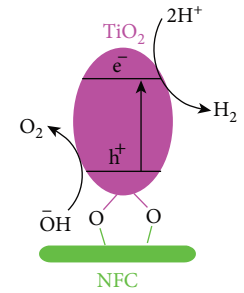


Figure 6: Deposition of $TiO_2$ on NFC as a catalyst for water splitting.

the hydrogen evolution reaction up to 287.2 $\mu$mol hr$^{-1}$ g$^{-1}$ [82]. NFC/$TiO_2$ was also modified by $Fe_3O_4$ NPs to produce a magnetic photocatalyst for the hydrogen evolution. For the synthesis of the catalyst, in situ generation of $Fe_3O_4$ NPs was carried out in NFC hydrogel, and the obtained nanocomposite was leached by $TiO_2$ NPs. In this work, $Fe_3O_4$ was employed as a shield of NFC against degradation by $TiO_2$ under UV irradiation which was needed for the hydrogen evolution reaction. This catalyst afforded up to 436 $\mu$mol g$^{-1}$ min$^{-1}$ hydrogen under photocatalytic conditions [83].

Zhang et al. [84] utilized doping polyaniline on bacterial Cel (BC) by the polymerization to construct a BC-covered polyaniline, and they compared the result of hydrogen evolution reaction by this system with the catalyst obtained from pyrolysis of BC/polyaniline. It seems hydrogen bonding and electrostatic interactions directly stabilized polyaniline on the BC. In both of the catalysts, microscopic studies revealed that the nanowire structures of BC were lost. These supports after deposition of Pt NPs were employed in the hydrogen generation in acidic media, in which Pt on the carbon support indicated better performance with the onset potential of

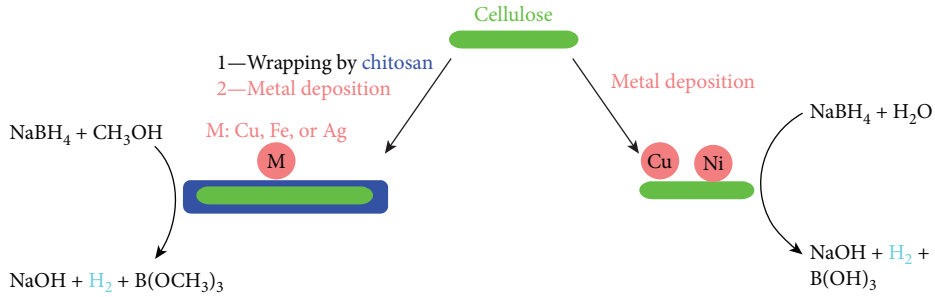


Scheme 10: Cu/Ni supported on Cel as a catalyst for the hydrolysis of $NaBH_4$ and Cel wrapped CS modified with metals as catalysts for the methanolysis of $NaBH_4$.

$-1\,mA\,cm^{-2}$ and overpotential of $-10\,mA\,cm^{-2}$, and Tafel slope of $-35\,mV\,dec^{-1}$ [84]. While Cel has been deprived from the strength ligands like amines (unlike CS), nevertheless hydroxyl groups could be weakly anchored to the metals. Hydrogel of wheat straw Cel was modified by nickel and copper NPs to construct two heterogeneous catalysts of hydrogen production from $NaBH_4$ with the rate up to $489.2\,\mu mol\,g^{-1}\,hr^{-1}$. This hydrogel was prepared by the polymerization in a solution, in which fine particles were formed as a support of the metal NPs. Kinetic study demonstrated that the hydrolysis reaction of $NaBH_4$ needs an $E_a$ of $32.66\,kJ\,mol^{-1}$. It was also indicated that the composite could be used up to five times with 100% conversion and 77.5% activity for hydrogen generation. The stability of the catalyst was investigated for a long time by storing it for 30 days, indicating that the stored catalyst retained activity of 70% for nickel composite and 65% for copper composite [85]. In another work, electroless deposition of Ni-P NPs on bacterial Cel (BC) was done. The Ni-P/BC electrode shows good HER performance with an overpotential of 161 mV at $10\,mA\,cm^{-2}$ and a Tafel slope of $141\,mV\,dec^{-1}$. The major advantages of this catalyst are low cost and easy fabrication [96]. CS-wrapped Cel composite grafted metal NPs, including copper, iron, and silver, to construct new catalysts of hydrogen evolution and remove organic pollutants (Scheme 10). Among the metals, Cu showed high activity on the biopolymer for the hydrogen generation from methanolysis of sodium borohydride. Rate of $1{,}253\,ml\,g^{-1}\,min^{-1}$ was obtained by the Cu catalyst as the stable and reusable one at ambient conditions [86]. It should be noted that the Cu has a remarkable tendency to coordinate with the Cel hydroxyl groups, leading to the dissolving the biopolymer by one of the known reagents as the Schweitzer solution ($Cu(NH_3)_4(OH)_2$).

Cel fibers were also modified by cadmium sulfide simply by an impregnation method. In this study, cadmium sulfide nanocrystals were deposited into the micropores of commercial Cel fiber. While the photocatalytic activity of the composite did not investigate, authors claimed that the perched semiconductor would be a promising photocatalyst for the water-splitting [97]. After that, the construction of a semiconductor using CdS, $MoS_2$, and BC was examined to reveal the impacts of each of the ingredients in the hydrogen evolution reaction. For the synthesis of the catalyst, BC aerogel and $MoS_2$ was simply combined, and CdS was added to them. Aerogel nature of the biopolymer led to the superior surface area of the final catalyst. Binding energies were calculated for various combinations of the three ingredients, in which CdS/10%$Mo_2S$ and CdS/10%BC-$Mo_2S$ afforded the less amounts (2.2 eV) as the desirable ones for the photocatalytic reactions. Evaluation of hydrogen evolution reaction by the synthesized catalysts revealed CdS/10%BC-$Mo_2S$ is the best composite with the hydrogen production rate of $20.02\,mmol\,hr^{-1}\,g^{-1}$ [87]. A super hydrophilic/superaerophobic $MoS_2$ catalyst with 3D conductive networks has been prepared, assisted with Cel nanofiber (CF) and carboxylated multi-walled carbon nanotubes (cMWCST). The resulting CF/cMWCST/$MoS_2$ catalyst showed excellent HER performance with an overpotential of 154 mV at $10\,mA\,cm^{-2}$. This result was due to its 3D network structure and which can disperse $MoS_2$ and cMWCST [98].

The potential of Cel in the supporting metal oxides has been attracted attentions to employ the biopolymer as the template of catalysts, considering that Cel is easily removed by a thermal treatment. Since the polymer is deconstructed to gases like $CO_2$, $H_2O$, and CO under high temperatures, the decomposition of the catalyst with Cel template created tremendous porosity in the catalyst structure due to the emission of the generated gases from Cel degradation. As an instance, 3D CS as the template of $TiO_2$ produced a promising organometallic compound for the final synthesis of anatase $TiO_2$ with a superior porosity observed by the Scanning Electron Microscopy. Furthermore, traces of carbon remained in the titania structure, which led to the enhancement in the visible light absorption by the semiconductor. This carbon doping leads to the decreasing energy gap between the valance band and the conduction band of titania. Water-splitting was conducted by this catalyst under photoelectrochemical conditions with the current density of up to $1.61\,mA\,cm^{-2}$ [99]. Cel was reconstructed to N-doped carbon materials in the presence of an amine, and Pt NPs were loaded on the obtained compound *via* atomic layer deposition. The use of the BC as the starting material of carbon compound has the advantages of providing high surface area, a fact that could be found from the electron microscopy imaging in this report. The catalyst carried out the water-splitting with the overpotential of $-55\,mV$ at the current density of $10\,mA\,cm^{-2}$ and Tafel slope of $32\,mV\,dec^{-1}$ [88].

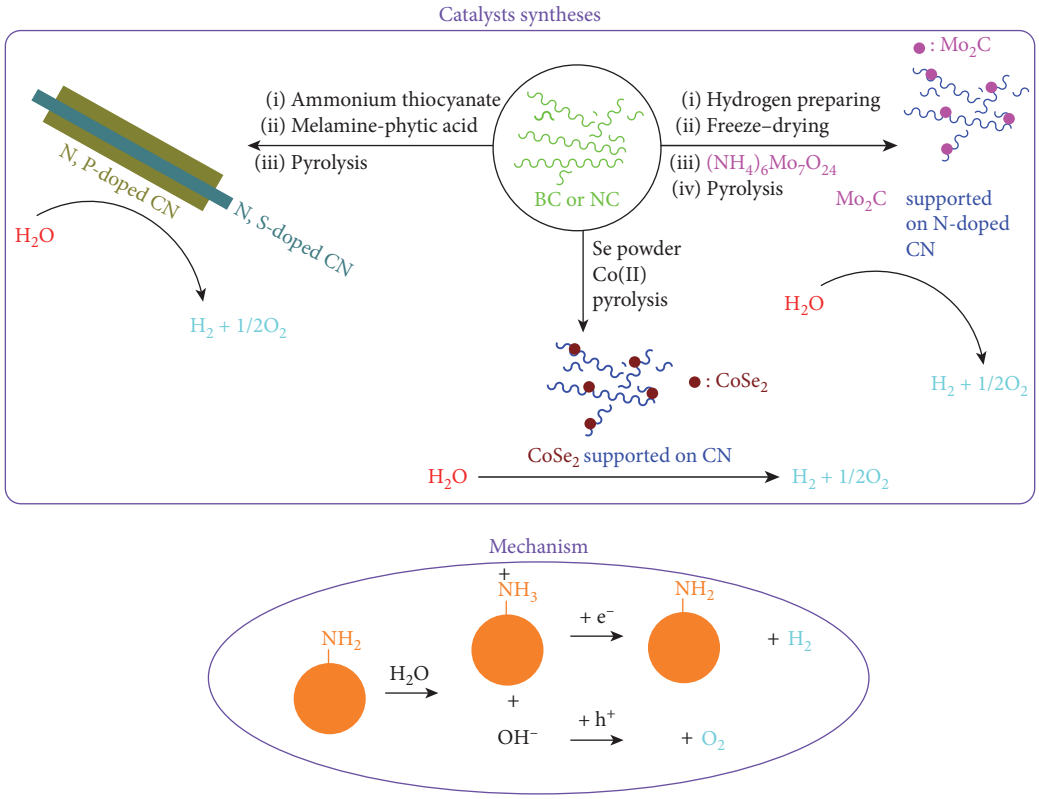


Scheme 11: Use of Cel derivatives as a starting material for CS-based catalysts for hydrogen generation.

The potential of Cel as the carbon materials precursor was employed to construct molybdenum carbide NPs deposited on 3D N-doped carbon nanofiber for the catalytic purpose in hydrogen evolution. This catalyst was obtained from BC in two steps, including (1) preparing hydrogel of Cel and subsequent freeze–drying to form a porous network and (2) pyrolysis of the first step product in the presence of $(NH_4)_6Mo_7O_{24}$. Electron microscopy study revealed the formation of an aerogel structure of N-doped carbons with the embedded $Mo_2C$ NPs. This non-noble catalyst successfully promoted the water-splitting with an overpotential of 167 mV at the current density of 10 mA $cm^{-2}$ and a high exchange current density of $4.73 \times 10^{-2}$ mA $cm^{-2}$. Notably, molybdenum carbide NPs decorated on 3D N-doped carbon nanofiber were stable in acidic media and conducted on the reaction in neutral and basic media. It was theoretically demonstrated that N-doped carbon nanofibers efficiently participate in the hydrogen evolution reaction accompanied with $Mo_2C$ [100]. This finding also confirms our previous claim about the role of nitrogen atoms in the evolution of proton to $H_2$. Carbon nanofibers hydrogel containing sulfate ester groups hydrolysis with $(NH_4)_6Mo_7O_{24}$, freeze-drying, and pyrolysis gave $Mo_2C$ supported on S-doped carbon aerogel as the catalyst for the hydrogen generation with an overpotential of 176 mV. The sulfate groups were loaded on the carbon nanofibers synthesis procedure from sulfuric acid hydrolysis [101]. A metal-free system based on multielements doped carbon nanomaterial was synthesized through carbon nanofibers impregnations by ammonium thiocyanate and melamine-phytic acid in two separate steps and pyrolysis of the achieved composite. A 3D network of N, S-doped carbon nanofibers coated with N, P-doped carbon NPs was obtained as a catalyst for the water-splitting. This catalyst progressed hydrogen evolution with the onset potential of 233 mV, a current density of 10 mA $cm^{-2}$ at 331 mV, and Tafel slope of 99 mV $dec^{-1}$. The conductivity of the carbon nanofibril support and the presence of active sites of N and P and their interactions with the N and S in the down level positively impressed the reaction [89].

Pyrolysis of BC afforded carbon nanofibers which under grown of $CoSe_2$ by a hydrothermal pathway, provided a 3D porous structure containing $CoSe_2$ NPs. This one-pot reaction led to the formation of a large surface area support for $CoSe_2$, leading to the abundance in the reaction sites and accessibility of them. Meanwhile, carbon nanofibers promoted the conductivity and electron transfer, a significant factor for achieving a high rate of hydrogen evolution reaction. Catalyzing water-splitting by the catalyst demonstrated a low onset overpotential of −85 mV, low overpotential ($\eta_{10} = 119$ mV) at a current density of −10 mA $cm^{-2}$ and smaller Tafel slope of 54 mV $dec^{-1}$ (Scheme 11) [90].

A new photocatalytic system was also obtained by hydrothermal treatment of the BC and CdS and then the addition of thiourea and ammonium molybdite. A berry-shaped-CdS was the product of the first stage, which under the second stage produced berry-shaped-CdS/$Mo_2S$ as the hydrogen generation reaction with the rate of 63.59 mmol $hr^{-1}$ $g^{-1}$. In this synthesis procedure, BC is utilized as a template with the

responsibility of molding the CdS NPs and an inhibitor of the NPs aggregation [91]. The decomposition of Cel could be employed for the carbon-doping reaction into other structures like graphitic carbon nitride. This reaction was conducted on for enhancing the optical properties of the graphitic carbon nitride for the photocatalytic agenda. Surprisingly, the carbon-doped semiconductor demonstrated an improvement in the photocatalytic hydrogen generation reaction 17 times better than the undoped one. It was found that a remarkable charge separation and photo-absorption was occurred, which both electronic and optical enhancement have positive on the hydrogen generation (up to $1.024\,\text{mmol}\,\text{hr}^{-1}\,\text{g}^{-1}$) [92].

## 6. Advantages, Limitations, and Prospectives of CS, Chitin, and Cel in Hydrogen Production

As the result of the mentioned reports on CS, chitin, and Cel, it can be concluded that these biopolymers could efficiently fill the gap of supports in the absence of harmful synthetic polymers. All of them provide a heterogeneous system for the photo, electrocatalytic, and photoelectrocatalytic hydrogen generation reactions on account of insolubility in the majority of the solvents. An abundance of active functional groups also creates an ideal opportunity to load various organic and inorganic compounds on them. Moreover, the surface area of CS and Cel could easily expanded by conversion of them to aerogel form to stablish more reaction sites, which finally increases the rate of hydrogen generation. The most fascinating common feature of CS, chitin, and Cel is the possibility of their transformation to carbon materials, in which a substantial enhancement is accommodated in the charge transfer as well as charge recombination retarding. By this structural revolution, the role of support is extended to semiconductor as well. This change and improvement was considerable, especially in chitosan with affording N-doped carbon materials. In addition, the known advantages of the biopolymers, such as inexpensive natures, accessibility, and safety, more highlight the role of them in the future of hydrogen energy.

Despite the mentioned benefits, the nonconductive nature of Cel is a drawback since the conducting polymers showed better performance with easy electron movement, especially in electrocatalytic and photoelectrocatalytic reactions. Furthermore, CS is dissolved in acidic moiety, leading to the deconstruction of catalyst when hydrogen generating in low pH like in formic acid. A common limitation for CS, chitin, and Cel is the low-temperature stability, limiting their applications at the high temperatures.

The COVID-19 pandemic had a significant impact on the global energy system and displayed the need for a sustainable energy sector. The pandemic reduced energy demand and oil price, which was an opportunity to the extension of renewable energy sources. Hydrogen is an energy carrier that can be produced from a variety of sources and used in many applications. Its role in energy systems is important because human need a cleaner and sustainable energy sector. This means that hydrogen has the potential to be a zero-emissions fuel, which could help reduce greenhouse gas emissions, and climate change [2, 102]. It was demonstrated that biopolymers-supported transition metals could be worthy catalysts for the generation of hydrogen. Their structures have the required potential to be modified to desired one for obtaining higher performance.

## 7. Conclusion and Perspective

CS, chitin, and Cel indicated considerable merits to be used in the fabrication of catalysts for hydrogen evolution reactions. The application of chitin has not been well established due to the lazy nitrogen atoms as the amide functionality, diminishing its anchoring to transition metals. Among them, CS was more studied due to the easy modification with the transition metals, acting as the weak base, efficient hydrogen bonding, charge recombination retarding, and facile transforming to valuable nitrogen-doped carbon. All of these are owed to the active amines on the backbone of this biopolymer. While cellulose does not contain nitrogen atoms, its modification with transition metals afforded powerful catalysts. This inexpensive natural polymer also afforded high surface area materials and carbon species as the supports of catalysts. However, we believe that the following perspective could be considered for the introduction of new catalysts based on these biopolymers:

(i) Modification of the biopolymers by active organometallic compounds like metallo phthalocyanines; (ii) use of porous forms of them like CS aerogel or Cel aerogel to provide high surface area catalysts; (iii) modification with other active transition metals, especially for chitin and C; (iv) developing new composites by the optically active materials, such as $TiO_2$, graphene derivatives, and quantum dots, to drive the hydrogen generation reaction photocatalytically.

Overall, there is a massive gap in the use of these susceptible biopolymers in the designing new catalysts in energy conversion; in particular, Cel and chitin-based catalysts have not been well established.

## Data Availability

The data used to support the findings of this study are available from the corresponding author upon request.

## Conflicts of Interest

The authors declare that they have no conflicts of interest.

## Authors' Contributions

Sajjad Keshipour contributed to the conceptualization, data curation, funding acquisition, project administration, writing—original draft, writing—review and editing; Mina Hadidi contributed to the conceptualization, data curation, writing—original draft, writing—review and editing; Ozra Gholipour contributed to the writing—review and editing.

## Acknowledgments

Authors gratefully acknowledge supports of the Research Councils of the Urmia University.

## References


[1] G. Ali-Mansoori, L. Barnie-Agyarko, L. Antonio-Estevez et al., "Fuels of the future for renewable energy sources (ammonia, biofuels, hydrogen)," Applied Physics, 2021.

[2] A. T. Hoang, S. Nižetić, A. I. Olcer et al., "Impacts of COVID-19 pandemic on the global energy system and the shift progress to renewable energy: opportunities, challenges, and policy implications," *Energy Policy*, vol. 154, Article ID 112322, 2021.

[3] M. A. Rosen and S. Koohi-Fayegh, "The prospects for hydrogen as an energy carrier: an overview of hydrogen energy and hydrogen energy systems," *Energy, Ecology and Environment*, vol. 1, pp. 10–29, 2016.

[4] A. Pareek, R. Dom, J. Gupta, J. Chandran, V. Adepu, and P. H. Borse, "Insights into renewable hydrogen energy: recent advances and prospects," *Materials Science for Energy Technologies*, vol. 3, pp. 319–327, 2020.

[5] S. Mousavi-Salehi, S. Keshipour, and F. Ahour, "Gold supported on graphene oxide/silica photocatalyst for hydrogen generation from formic acid," *Journal of Physics and Chemistry of Solids*, vol. 176, Article ID 111239, 2023.

[6] A. Al-Azmi and S. Keshipour, "New bidental sulfur-doped graphene quantum dots modified with gold as a catalyst for hydrogen generation," *Journal of Colloid and Interface Science*, vol. 612, pp. 701–709, 2022.

[7] S. Keshipour and S. Mohammad-Alizadeh, "Nickel phthalocyanine@graphene oxide/$TiO_2$ as an efficient degradation catalyst of formic acid toward hydrogen production," *Scientific Reports*, vol. 11, Article ID 16148, 2021.

[8] S. Keshipour, S. Mohammad-Alizadeh, and M. H. Razeghi, "Copper phthalocyanine@graphene oxide as a cocatalyst of $TiO_2$ in hydrogen generation," *Journal of Physics and Chemistry of Solids*, vol. 161, Article ID 110434, 2022.

[9] A. Al-Azmi and S. Keshipour, "Cross-linked chitosan aerogel modified with Pd(II)/phthalocyanine: synthesis, characterization, and catalytic application," *Scientific Reports*, vol. 9, Article ID 13849, 2019.

[10] S. Keshipour and K. Adak, "Magnetic d-penicillamine-functionalized cellulose as a new heterogeneous support for cobalt(II) in green oxidation of ethylbenzene to acetophenone," *Applied Organometallic Chemistry*, vol. 31, no. 11, Article ID e3774, 2017.

[11] C. Wang, T. Yokota, and T. Someya, "Natural biopolymer-based biocompatible conductors for stretchable bioelectronics," *Chemical Reviews*, vol. 121, no. 4, pp. 2109–2146, 2021.

[12] A. Sharma, M. Thakur, M. Bhattacharya, T. Mandal, and S. Goswami, "Commercial application of cellulose nanocomposites—a review," *Biotechnology Reports*, vol. 21, Article ID e00316, 2019.

[13] D. Lavanya, P. K. Kulkarni, M. Dixit, P. K. Raavi, and L. N. V. Krishna, "Sources of cellulose and their applications—a review," *International Journal of Drug Formulation and Research*, vol. 2, no. 6, pp. 19–38, 2011.

[14] H. Seddiqi, E. Oliaei, H. Honarkar et al., "Cellulose and its derivatives: towards biomedical applications," *Cellulose*, vol. 28, pp. 1893–1931, 2021.

[15] A. Shabrandi, S. Azizi, R. Hobbenaghi, A. Ownagh, and S. Keshipour, "The healing effect of chitosan supported nano-$CeO_2$ on experimental excisional wound infected with *Pseudomonas aeruginosa* in rat," *Iranian Journal of Veterinary Surgery*, vol. 12, no. 2, pp. 9–20, 2017.

[16] M. Nasrollahzadeh, N. Shafiei, Z. Nezafat, N. S. S. Bidgoli, and F. Soleimani, "Recent progresses in the application of cellulose, starch, alginate, gum, pectin, chitin and chitosan based (nano) catalysts in sustainable and selective oxidation reactions: a review," *Carbohydrate Polymers*, vol. 241, Article ID 116353, 2020.

[17] W.-H. Chen, P. P. Biswas, H. C. Ong, A. T. Hoang, T.-B. Nguyen, and C.-D. Dong, "A critical and systematic review of sustainable hydrogen production from ethanol/bioethanol: steam reforming, partial oxidation, and autothermal reforming," *Fuel*, vol. 333, Part 2, Article ID 126526, 2023.

[18] A. T. Hoang, Z. H. Huang, S. Nižetić et al., "Characteristics of hydrogen production from steam gasification of plant-originated lignocellulosic biomass and its prospects in Vietnam," *International Journal of Hydrogen Energy*, vol. 47, no. 7, pp. 4394–4425, 2022.

[19] N. Imanuella, T. Witoon, Y. W. Cheng et al., "Interfacial-engineered $CoTiO_3$-based composite for photocatalytic applications: a review," *Environmental Chemistry Letters*, vol. 20, pp. 3039–3069, 2022.

[20] K. C. Christoforidis and P. Fornasiero, "Photocatalytic hydrogen production: a rift into the future energy supply," *ChemCatChem*, vol. 9, no. 9, pp. 1523–1544, 2017.

[21] S. Guo, X. Li, J. Li, and B. Wei, "Boosting photocatalytic hydrogen production from water by photothermally induced biphase systems," *Nature Communications*, vol. 12, Article ID 1343, 2021.

[22] Y. Li, X. Wei, L. Chen, and J. Shi, "Electrocatalytic hydrogen production trilogy," *Angewandte Chemie International Edition*, vol. 60, no. 36, pp. 19550–19571, 2021.

[23] S. Anwar, F. Khan, Y. Zhang, and A. Djire, "Recent development in electrocatalysts for hydrogen production through water electrolysis," *International Journal of Hydrogen Energy*, vol. 46, no. 63, pp. 32284–32317, 2021.

[24] H. Narayanan, B. Viswanathan, K. R. Krishnamurthy, and H. Nair, "Hydrogen from photo-electrocatalytic water splitting," in *Solar Hydrogen Production Processes, Systems and Technologies*, F. Calise, M. D. D'Accadia, M. Santarelli, A. Lanzini, and D. Ferrero, Eds., pp. 419–486, Academic Press, 2019.

[25] P. M. Adamopoulos, I. Papagiannis, D. Raptis, and P. Lianos, "Photoelectrocatalytic hydrogen production using a $TiO_2$/$WO_3$ bilayer photocatalyst in the presence of ethanol as a fuel," *Catalysts*, vol. 9, no. 12, Article ID 976, 2019.

[26] A. T. Hoang, A. Pandey, W.-H. Chen et al., "Hydrogen production by water splitting with support of metal and carbon-based photocatalysts," *ACS Sustainable Chemistry & Engineering*, vol. 11, no. 4, pp. 1221–1252, 2023.

[27] V. Kumaravel, M. D. Imam, A. Badreldin et al., "Photocatalytic hydrogen production: role of sacrificial reagents on the activity of oxide, carbon, and sulfide catalysts," *Catalysts*, vol. 9, no. 3, Article ID 276, 2019.

[28] T. S. Teets and D. G. Nocera, "Photocatalytic hydrogen production," *Chemical Communications*, vol. 47, no. 33, pp. 9268–9274, 2011.

[29] F. Deng, J.-P. Zou, L.-N. Zhao, G. Zhou, X.-B. Luo, and S.-L. Luo, "Nanomaterial-based photocatalytic hydrogen production," in *Nanomaterials for the Removal of Pollutants and Resource Reutilization Micro and Nano Technologies*, X. Luo and F. Deng, Eds., pp. 59–82, Elsevier, 2019.

[30] R. Li and C. Li, "Photocatalytic water splitting on semiconductor-based photocatalysts," in *Advances in Catalysis*, C. Song, Ed., vol. 60, pp. 1–57, Academic Press, 2017.

[31] C. G. Margarit, N. G. Asimow, A. E. Thorarinsdottir, C. Costentin, and D. G. Nocera, "Impactful role of cocatalysts on molecular electrocatalytic hydrogen production," *ACS Catalysis*, vol. 11, no. 8, pp. 4561–4567, 2021.

[32] C. Wang, H. Shang, L. Jin, H. Xu, and Y. Du, "Advances in hydrogen production from electrocatalytic seawater splitting," *Nanoscale*, vol. 13, no. 17, pp. 7897–7912, 2021.

[33] S. Wang, A. Lu, and C.-J. Zhong, "Hydrogen production from water electrolysis: role of catalysts," *Nano Convergence*, vol. 8, Article ID 4, 2021.

[34] G. Li, G. Han, L. Wang et al., "Dual hydrogen production from electrocatalytic water reduction coupled with formaldehyde oxidation via a copper–silver electrocatalyst," *Nature Communications*, vol. 14, Article ID 525, 2023.

[35] M. Ye, J. Gong, Y. Lai, C. Lin, and Z. Lin, "High-efficiency photoelectrocatalytic hydrogen generation enabled by palladium quantum dots-sensitized $TiO_2$ nanotube arrays," *Journal of the American Chemical Society*, vol. 134, no. 38, pp. 15720–15723, 2012.

[36] A. Mehtab, S. M. Alshehri, and T. Ahmad, "Photocatalytic and photoelectrocatalytic water splitting by porous g-$C_3$ $N_4$ nanosheets for hydrogen generation," *ACS Applied Nano Materials*, vol. 5, no. 9, pp. 12656–12665, 2022.

[37] L. Nagy, R. González-Gómez, G. K. Dinesh, and P. Farràs, "Photoelectrocatalytic $H_2$ production," in *Photocatalytic Hydrogen Production for Sustainable Energy*, A. Puga, Ed., pp. 95–121, John Wiley & Sons, Ltd, 2023.

[38] J. Yu, C. Gong, Z. Wu et al., "Efficient visible light-induced photoelectrocatalytic hydrogen production using CdS sensitized $TiO_2$ nanorods on $TiO_2$ nanotube arrays," *Journal of Materials Chemistry A*, vol. 3, no. 44, pp. 22218–22226, 2015.

[39] M. Fedel, F. Parrino, and S. Scirè, *Photoelectrocatalysis*, Elsevier, 2023.

[40] V. Vijayalekshmi and D. Khastgir, "Fabrication and comprehensive investigation of physicochemical and electrochemical properties of chitosan-silica supported silicotungstic acid nanocomposite membranes for fuel cell applications," *Energy*, vol. 142, pp. 313–330, 2018.

[41] F. Eyvari-Ashnak and S. Keshipour, "Amines functionalities on chitosan boasting photocatalytic activity of cobalt (II)-phthalocyanine in water-splitting," *Molecular Catalysis*, vol. 534, Article ID 112820, , 2023.

[42] S. Bahadar Khan, M. S. Javed Khan, E. M. Bakhsh, K. Akhtar, and A. M. Asiri, "Metallic nanoparticles decorated chitosan hydrogel wrapped pencil graphite: Effective catalyst for reduction of water pollutants and hydrogen production," *Surfaces and Interfaces*, vol. 31, Article ID 102004, 2022.

[43] F. Azimi, A. P. Marjani, and S. Keshipour, "Fe(II)-phthalocyanine supported on chitosan aerogel as a catalyst for oxidation of alcohols and alkyl arenes," *Scientific Reports*, vol. 11, Article ID 23769, 2021.

[44] N. Kalanpour, S. Nejati, and S. Keshipour, "Pd nanoparticles/graphene quantum dot supported on chitosan as a new catalyst for the reduction of nitroarenes to arylamines," *Journal of the Iranian Chemical Society*, vol. 18, pp. 1243–1250, 2021.

[45] M. J. González-Pabón, R. Cardeña, E. Cortón, and G. Buitrón, "Hydrogen production in two-chamber MEC using a low-cost and biodegradable poly(vinyl) alcohol/chitosan membrane," *Bioresource Technology*, vol. 319, Article ID 124168, 2021.

[46] X. Chen, X.-J. Xu, X.-C. Zheng, X.-X. Guan, and P. Liu, "Chitosan supported palladium nanoparticles: the novel catalysts for hydrogen generation from hydrolysis of ammonia borane," *Materials Research Bulletin*, vol. 103, pp. 89–95, 2018.

[47] M. Cao, Y. Liu, S. Zhang, Z. Wang, and S. Xu, "Synthesis and photocatalytic hydrogen evolution properties of chitosan cobalt complex," *Chemical Journal of Chinese Universities*, vol. 41, no. 4, Article ID 735, 2020.

[48] E. M. Bakhsh, M. S. J. Khan, K. Akhtar, S. B. Khan, and A. M. Asiri, "Chitosan hydrogel wrapped bimetallic nanoparticles based efficient catalysts for the catalytic removal of organic pollutants and hydrogen production," *Applied Organometallic Chemistry*, vol. 36, no. 7, Article ID e6741, 2022.

[49] Y. Pi, X. Wu, Z. Zheng, L. Ma, and T. Wang, "Chitosan–lignin carbon framework-encapsulated Cu catalyst facilitates base-free hydrogen evolution from methanol/water," *Catalysis Science & Technology*, vol. 12, no. 6, pp. 1941–1949, 2022.

[50] Y. Liu, J. Mao, Y. Huang et al., "Pt-chitosan-$TiO_2$ for efficient photocatalytic hydrogen evolution via ligand-to-metal charge transfer mechanism under visible light," *Molecules*, vol. 27, no. 15, Article ID 4673, 2022.

[51] H. Jia, Y. Zhu, X. Song, X. Zheng, and P. Liu, "Magnetic graphene oxide-ionic liquid grafted chitosan composites anchored Pd(0) nanoparticles: a robust heterogeneous catalyst with enhanced activity and superior reusability for hydrogen generation from ammonia borane," *International Journal of Hydrogen Energy*, vol. 43, no. 43, pp. 19939–19946, 2018.

[52] R. F. N. Quadrado and A. R. Fajardo, "Hydrogen generation and hydrogenation reactions efficiently mediated by a thin film of reduced graphene oxide-grafted with carboxymethyl chitosan and Ag nanoparticles," *Journal of Colloid and Interface Science*, vol. 583, pp. 626–641, 2021.

[53] D. B. Kayan and D. Koçak, "Enhanced catalytic activity of ppy-coated pencil electrode in the presence of chitosan and Au nanoparticles for hydrogen evolution reaction," *Journal of Solid State Electrochemistry*, vol. 21, pp. 2791–2798, 2017.

[54] S. Bano, A. S. Ganie, R. I. A. Khan, S. Sultana, M. Z. Khan, and S. Sabir, "Designing and application of PPy/$Bi_2MoO_6$/chitosan nanocomposites for electrochemical detection of ciprofloxacin and benzene and evaluation of hydrogen evolution reaction." *Surfaces and Interfaces*, vol. 29, Article ID 101786, 2022.

[55] D. B. Kayan, D. Koçak, and M. İlhan, "The activity of PAni-Chitosan composite film decorated with Pt nanoparticles for electrocatalytic hydrogen generation," *International Journal of Hydrogen Energy*, vol. 41, no. 25, pp. 10522–10529, 2016.

[56] A. Nasri, B. Jaleh, S. Khazalpour, M. Nasrollahzadeh, and M. Shokouhimehr, "Facile synthesis of graphitic carbon nitride/chitosan/Au nanocomposite: a catalyst for electrochemical hydrogen evolution," *International Journal of Biological Macromolecules*, vol. 164, pp. 3012–3024, 2020.

[57] P. S. Kumar and P. Prakash, "Metal free nanocomposite of graphitic carbon nitride, boron nitride and chitosan for efficient evolution of hydrogen: a strategic approach to achieving sustainable and effective electrocatalysis," *Journal of Environmental Chemical Engineering*, vol. 11, no. 1, Article ID 109045, 2023.

[58] Z. Pu, M. Wang, Z. Kou, I. S. Amiinu, and S. Mu, "$Mo_2C$ quantum dot embedded chitosan-derived nitrogen-doped carbon for efficient hydrogen evolution in a broad pH range," *Chemical Communications*, vol. 52, no. 86, pp. 12753–12756, 2016.

[59] F. Karimi, E. E. Altuner, F. Gulbagca et al., "Facile biofabrication of ZnO@AC nanoparticles from chitosan: characterization, hydrogen generation, and photocatalytic properties," *Environmental Research*, vol. 216, Part 4, Article ID 114668, 2023.

[60] P. Guo, S. Yuan, B. Guo, S. Li, and Y. Gao, "Chitosan-derived carbon supported CoO combined with CdS facilitates visible light catalytic hydrogen evolution," *Catalysis Science & Technology*, vol. 13, no. 4, pp. 1128–1139, 2023.

[61] G. R. M. Tomboc, A. H. Tamboli, and H. Kim, "Synthesis of $Co_3O_4$ macrocubes catalyst using novel chitosan/urea template for hydrogen generation from sodium borohydride," *Energy*, vol. 121, pp. 238–245, 2017.

[62] E. Paleček and L. Římánková, "Chitosan catalyzes hydrogen evolution at mercury electrodes," *Electrochemistry Communications*, vol. 44, pp. 59–62, 2014.

[63] A. Anouar, N. Katir, A. El Kadib, A. Primo, and H. García, "Palladium supported on porous chitosan–graphene oxide aerogels as highly efficient catalysts for hydrogen generation from formate," *Molecules*, vol. 24, no. 18, Article ID 3290, 2019.

[64] S. A. Gawad, A. Nasr, A. M. Fekry, and L. O. Filippov, "Electrochemical and hydrogen evolution behaviour of a novel nano-cobalt/nano-chitosan composite coating on a surgical 316L stainless steel alloy as an implant," *International Journal of Hydrogen Energy*, vol. 46, no. 35, pp. 18233–18241, 2021.

[65] Y. Zhang, W. Zhou, L. Jia et al., "Visible light driven hydrogen evolution using external and confined CdS: effect of chitosan on carriers separation," *Applied Catalysis B: Environmental*, vol. 277, Article ID 119152, 2020.

[66] S. Keshipour, F. Ahmadi, and B. Seyyedi, "Chitosan-modified Pd(II)-*d*-penicillamine: preparation, characterization, and catalyst application," *Cellulose*, vol. 24, pp. 1455–1462, 2017.

[67] H. Sachdeva, "Recent advances in the catalytic applications of GO/rGO for green organic synthesis," *Green Processing and Synthesis*, vol. 9, no. 1, pp. 515–537, 2020.

[68] D. B. Kayan, M. İlhan, and D. Koçak, "Chitosan-based hybrid nanocomposite on aluminium for hydrogen production from water," *Ionics*, vol. 24, pp. 563–569, 2018.

[69] J. L. Shamshina, P. Berton, and R. D. Rogers, "Advances in functional chitin materials: a review," *ACS Sustainable Chemistry & Engineering*, vol. 7, no. 7, pp. 6444–6457, 2019.

[70] J. Zhang, F. Lin, L. Yang et al., "Ultrasmall Ru nanoparticles supported on chitin nanofibers for hydrogen production from $NaBH_4$ hydrolysis," *Chinese Chemical Letters*, vol. 31, no. 7, pp. 2019–2022, 2020.

[71] W. Liu, H. Zhu, L. Ying et al., "*In situ* synthesis of small Pt nanoparticles on chitin aerogel derived N doped ultra-thin carbon nanofibers for superior hydrogen evolution catalysis," *New Journal of Chemistry*, vol. 43, no. 42, pp. 16490–16496, 2019.

[72] P. Guo, Z. Xiong, S. Yuan, K. Xie, H. Wang, and Y. Gao, "The synergistic effect of Co/CoO hybrid structure combined with biomass materials promotes photocatalytic hydrogen evolution," *Chemical Engineering Journal*, vol. 420, Part 3, Article ID 130372, 2021.

[73] E. Ma, T. Shen, D. Ying et al., "Chitin derived carbon anchored ultrafine Ru nanoparticles for efficient hydrogen evolution reaction," *ACS Sustainable Chemistry & Engineering*, vol. 10, no. 47, pp. 15530–15537, 2022.

[74] S. Hamzehzad and S. Keshipour, "$TiO_2$/hydrophobic cellulose aerogel nanocomposite as a new photocatalyst for oxidation of alcohols and ethylbenzene," *International Journal of Nanoscience and Nanotechnology*, vol. 17, no. 4, pp. 231–238, 2021.

[75] R. Bahluli and S. Keshipour, "Microcrystalline cellulose modified with Fe(II)– and Ni(II)–phthalocyanines: syntheses, characterizations, and catalytic applications," *Polyhedron*, vol. 169, pp. 176–182, 2019.

[76] X. Liu, Y. Jiang, X. Song, C. Qin, S. Wang, and K. Li, "A biomechanical process for cellulose nanofiber production—towards a greener and energy conservation solution," *Carbohydrate Polymers*, vol. 208, pp. 191–199, 2019.

[77] T. G. M. van de Ven and A. Sheikhi, "Hairy cellulose nanocrystalloids: a novel class of nanocellulose," *Nanoscale*, vol. 8, no. 33, pp. 15101–15114, 2016.

[78] J. P. F. Carvalho, A. C. Q. Silva, A. J. D. Silvestre, C. S. R. Freire, and C. Vilela, "Spherical cellulose micro and nanoparticles: a review of recent developments and applications," *Nanomaterials*, vol. 11, no. 10, Article ID 2744, 2021.

[79] S. Keshipour and M. Khezerloo, "Nanocomposite of hydrophobic cellulose aerogel/graphene quantum dot/Pd: synthesis, characterization, and catalytic application," *RSC Advances*, vol. 9, no. 30, pp. 17129–17136, 2019.

[80] W. Zhou, Z. Wang, H. Huang et al., "Significant enhancement in hydrogen evolution rate of 2D bismuth oxychloride lamellar membrane photocatalyst with cellulose nanofibers," *Chemical Engineering Journal*, vol. 456, Article ID 140933, 2023.

[81] X. An, Y. Wen, A. Almujil et al., "Nano-fibrillated cellulose (NFC) as versatile carriers of $TiO_2$ nanoparticles (TNPs) for photocatalytic hydrogen generation," *RSC Advances*, vol. 6, no. 92, pp. 89457–89466, 2016.

[82] C. Wang, J. Li, E. Paineau et al., "A sol–gel biotemplating route with cellulose nanocrystals to design a photocatalyst for improving hydrogen generation," *Journal of Materials Chemistry A*, vol. 8, no. 21, pp. 10779–10786, 2020.

[83] X. An, D. Cheng, L. Dai et al., "Synthesis of nano-fibrillated cellulose/magnetite/titanium dioxide (NFC@$Fe_3O_4$@TNP) nanocomposites and their application in the photocatalytic hydrogen generation," *Applied Catalysis B: Environmental*, vol. 206, pp. 53–64, 2017.

[84] Y. Zhang, J. Tan, F. Wen et al., "Platinum nanoparticles deposited nitrogen-doped carbon nanofiber derived from bacterial cellulose for hydrogen evolution reaction," *International Journal of Hydrogen Energy*, vol. 43, no. 12, pp. 6167–6176, 2018.

[85] J. Ding, Q. Li, Y. Su, Q. Yue, B. Gao, and W. Zhou, "Preparation and catalytic activity of wheat straw cellulose based hydrogel-nanometal composites for hydrogen generation from $NaBH_4$ hydrolysis," *International Journal of Hydrogen Energy*, vol. 43, no. 21, pp. 9978–9987, 2018.

[86] S. B. Khan, "Metal nanoparticles containing chitosan wrapped cellulose nanocomposites for catalytic hydrogen production and reduction of environmental pollutants," *Carbohydrate Polymers*, vol. 242, Article ID 116286, 2020.

[87] J. Hao, X. Dai, J. Gao et al., "Synergistic enhancement effect of moisture and aging on frequency dielectric response of oil-immersed cellulose insulation and its degree of polymerization evaluation using dielectric modulus," *Cellulose*, vol. 28, pp. 1–17, 2021.

[88] T. Liu, Y.-F. Guo, Y.-M. Yan et al., "CoO nanoparticles embedded in three-dimensional nitrogen/sulfur co-doped carbon nanofiber networks as a bifunctional catalyst for oxygen reduction/evolution reactions," *Carbon*, vol. 106, pp. 84–92, 2016.

[89] A. Mulyadi, Z. Zhang, M. Dutzer, W. Liu, and Y. Deng, "Facile approach for synthesis of doped carbon electrocatalyst from cellulose nanofibrils toward high-performance

metal-free oxygen reduction and hydrogen evolution," *Nano Energy*, vol. 32, pp. 336–346, 2017.

[90] L. Wei, J. Luo, L. Jiang et al., "$CoSe_2$ nanoparticles grown on carbon nanofibers derived from bacterial cellulose as an efficient electrocatalyst for hydrogen evolution reaction," *International Journal of Hydrogen Energy*, vol. 43, no. 45, pp. 20704–20711, 2018.

[91] S. Jiang, Q. Hu, M. Xu et al., "Crystalline CdS/$MoS_2$ shape-controlled by a bacterial cellulose scaffold for enhanced photocatalytic hydrogen evolution," *Carbohydrate Polymers*, vol. 250, Article ID 116909, 2020.

[92] P. Deng, H. Li, Z. Wang, and Y. Hou, "Enhanced photocatalytic hydrogen evolution by carbon-doped carbon nitride synthesized via the assistance of cellulose," *Applied Surface Science*, vol. 504, Article ID 144454, 2020.

[93] M. S. Seehra, L. P. Akkineni, M. Yalamanchi, V. Singh, and J. Poston, "Structural characteristics of nanoparticles produced by hydrothermal pretreatment of cellulose and their applications for electrochemical hydrogen generation," *International Journal of Hydrogen Energy*, vol. 37, no. 12, pp. 9514–9523, 2012.

[94] H. Heidari, "Ag nanoparticle/nanofibrillated cellulose composite as an effective and green catalyst for reduction of 4-nitrophenol," *Journal of Cluster Science*, vol. 29, pp. 475–481, 2018.

[95] I. S. Martakov, M. A. Torlopov, V. I. Mikhaylov, E. F. Krivoshapkina, V. E. Silant'ev, and P. V. Krivoshapkin, "Interaction of cellulose nanocrystals with titanium dioxide and peculiarities of hybrid structures formation," *Journal of Sol-Gel Science and Technology*, vol. 88, pp. 13–21, 2018.

[96] W. Wang, S. Khabazian, M. Casas-Papiol et al., "Nanoarchitectonics of bacterial cellulose with nickel-phosphorous alloy as a binder-free electrode for efficient hydrogen evolution reaction in neutral solution," *International Journal of Hydrogen Energy*, vol. 47, no. 69, pp. 29753–29761, 2022.

[97] G. Graham Allan Daniel, D. L. Bauer, and W. Huang, "Cellulose-based synthesis of photocatalytic cadmium sulfide semiconductor nanocrystals within microporous fibers for generation of hydrogen from water and sunlight," *Cellulose Chemistry and Technology*, vol. 47, no. 1-2, pp. 1–4, 2013.

[98] M. Chen, S. Deng, Y. Qing et al., "Approaching well-dispersed $MoS_2$ assisted with cellulose nanofiber for highly durable hydrogen evolution reaction," *Carbohydrate Polymers*, vol. 294, Article ID 119754, 2022.

[99] Z. Li, C. Yao, Y. Yu, Z. Cai, and X. Wang, "Highly efficient capillary photoelectrochemical water splitting using cellulose nanofiber-templated $TiO_2$ photoanodes," *Advanced Materials*, vol. 26, no. 14, pp. 2262–2267, 2014.

[100] Z.-Y. Wu, B.-C. Hu, P. Wu et al., "$Mo_2C$ nanoparticles embedded within bacterial cellulose-derived 3D N-doped carbon nanofiber networks for efficient hydrogen evolution," *NPG Asia Materials*, vol. 8, Article ID e288, 2016.

[101] X. Kong, S. Chen, Y. Zou et al., "Cellulose nanocrystals (CNC) derived $Mo_2C$@sulfur-doped carbon aerogels for hydrogen evolution," *International Journal of Hydrogen Energy*, vol. 43, no. 30, pp. 13720–13726, 2018.

[102] L. Fan, Z. Tu, and S. H. Chan, "Recent development of hydrogen and fuel cell technologies: A review," *Energy Reports*, vol. 7, pp. 8421–8446, 2021.